

## RESEARCH OUTCOME

### SELECTED ABSTRACTS

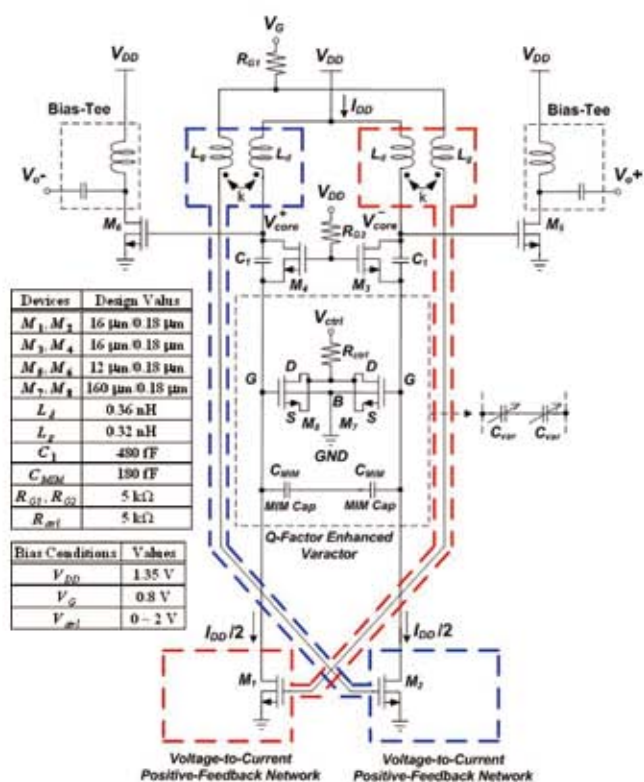
#### MMIC / RFIC

- A K-band low-power Colpitts VCO with voltage-to-current positive-feedback network in 0.18- $\mu\text{m}$  CMOS

T. -P. Wang

*IEEE Microw. Wireless Comp. Lett.*, vol. 21, no. 4, pp. 218-220, Apr. 2011.

A circuit topology suitable for low-power Colpitts voltage-controlled oscillators (VCOs) is presented in this letter. By employing the proposed voltage-to-current positive-feedback network, the required transconductance for VCO startup can be reduced, leading to the minimized dc power for sustaining VCO oscillation. Moreover, the Q-factor enhanced varactor is used in this VCO design for phase noise improvement. Based on the proposed architecture, the fabricated VCO in standard 0.18- $\mu\text{m}$  CMOS exhibits a 3.58% tuning range. Operating at 1.35-V supply voltage, the VCO core consumes 3.3-mW dc power. The measured phase noise is -110.82 dBc/Hz at 1-MHz offset from 18.95-GHz oscillation frequency. Compared with the recently published K-band 0.18- $\mu\text{m}$  CMOS VCOs, it is observed that the proposed Colpitts VCO exhibits comparable circuit performance under low dc-power consumption.

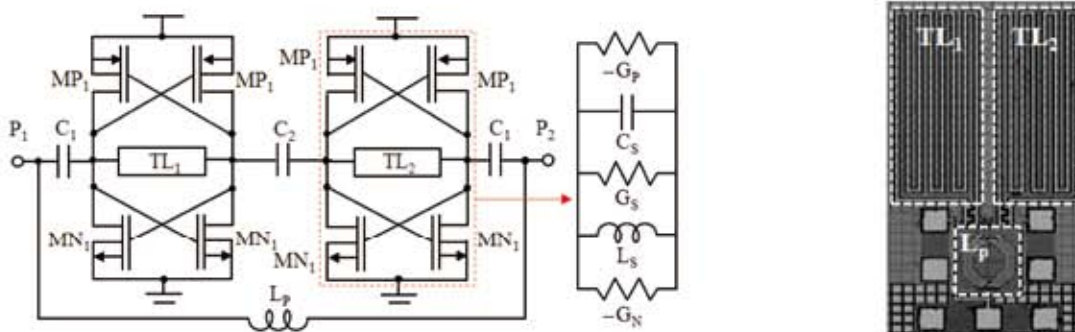


■ Design of CMOS active bandpass filter with three transmission zeros

S. Wang, and B.-Z. Huang

*Electron. Lett.*, Vol.47, No. 20, pp. 1030-1031, Sep., 2011.

An active bandpass filter with three transmission zeros is proposed. The filter consists of complementary cross-couple pairs to compensate resistive losses of resonators and a shunt-feedback inductor (LP) to achieve the transmission zeros. The circuit is designed, implemented, and verified in a standard 0.18- $\mu\text{m}$  CMOS process. The circuit with a chip size of  $0.55 \times 0.9 \text{ mm}^2$  draws 2.4 mA from a 2.1-V supply voltage. The measured insertion and return loss at 11 GHz is 1.7 dB and 26 dB. The rejection levels at these transmission zeros are greater than 12 dB. Moreover, the introduction of LP demonstrates a 1.8-dB and 2.5-dB improvement in NF and linearity compared to the filter without LP.

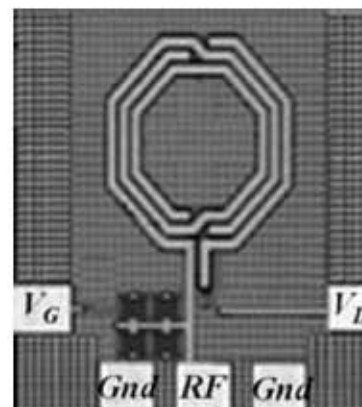
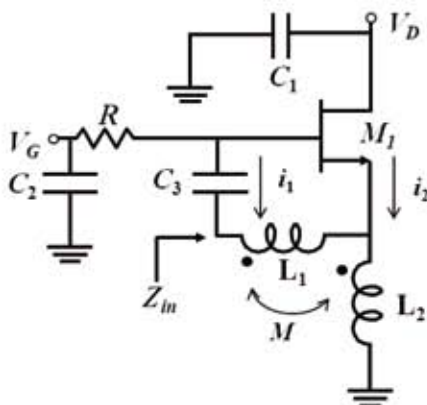


■ Q-enhanced CMOS inductor using tapped-inductor feedback

S. Wang, and R.-X. Wang

*Electron. Lett.*, Vol.47, No. 16, pp. 921-922, Aug., 2011.

A Q-enhanced inductor using tapped-inductor feedback technique is presented. Compared with conventional transformer feedback architectures, this proposed technique not only compensates resistive losses with low-power consumption but also provides a high-inductance inductor. The inductor which consists of a NMOS transistor, a capacitor, and a tapped inductor is implemented in a standard 0.18- $\mu\text{m}$  CMOS process. The measured resistance is about  $1.0 \Omega$  at 3 GHz. And the 3.9-nH semi-passive inductor with a measured Q peak of 74.2 around 3 GHz is also demonstrated. The semi-passive inductor draws 1.5 mA from a 0.8-V supply voltage while the chip size is  $0.5 \times 0.56 \text{ mm}^2$  including all testing pads.



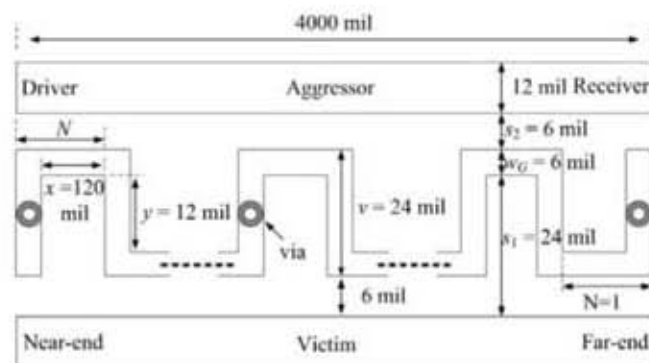
## Signal Integrity and Packaging

### ■ Suppression Of Crosstalk Using Serpentine Guard Trace Vias

W.-T. Huang, C.-H. Lu, and D.-B. Lin

*Progress In Electromagn. Research*, vol. 109, 37-61, 2010.

The proposed serpentine guard trace via (SGTV) structure which uses grounded vias on the serpentine guard trace (SGT) to provide effective suppression of both near-end crosstalk (NEXT) and far-end crosstalk (FEXT) simultaneously. Unlike the SGT approach, which requires extra components on the guard trace and can suppress only FEXT, our design uses vias and suppresses both NEXT and FEXT. We have proposed a design rule to determine the total length and the horizontal section length of the trace to achieve optimum performance. In addition, we developed a method for determining the number and spacing of vias to achieve the desired bandwidth. Together, these can be used to quickly create the SGTV structure. The suppression of NEXT and FEXT is quite effective and our design may be used in practical engineering solutions.



## Antenna

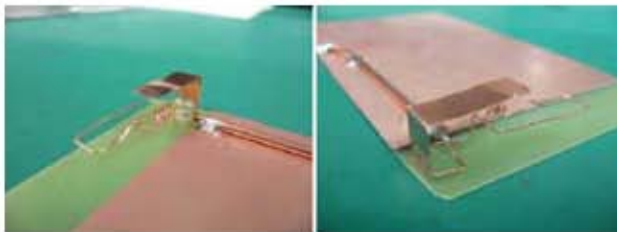
### Cellular Antenna Design and Measurement

C.-P. Chou<sup>1</sup>, J.-S. Sun<sup>1</sup>, Y.-D. Chen<sup>2</sup>, and G.-Y. Chen<sup>1</sup>

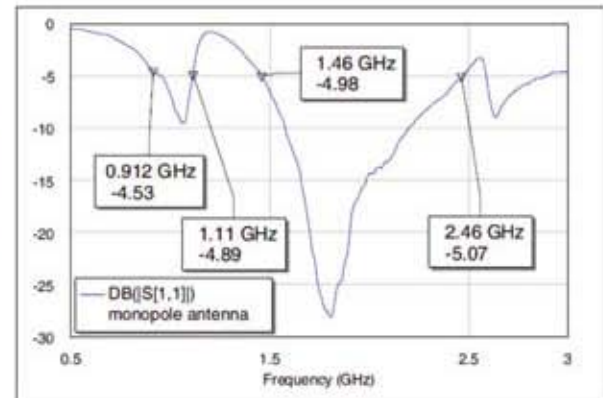
<sup>1</sup>Department of Electronic Engineering, National Taipei University of Technology, Taiwan

<sup>2</sup>Antenna and EMC Laboratory, HTC Corporation, Taiwan

A high performance monopole antenna is designed. A prototype of the proposed monopole antenna with a compact area size is implemented, and the antenna shows a wide operating bandwidth for low band and high band bandwidth, making it easy to cover the GSM, EDGE, CDMA, CDMA 2000, W-CDMA and UMTS band for wireless communication and 2.5G/3G dual mode operation of a mobile handset phone.



Dual wideband monopole antenna design



Measured data of return loss

Frequency (MHz)	800	850	900	950	1000	1500	1600	1700
Directivity (dBi)	3.41	3.83	3.31	4.26	3.51	5.35	4.06	4.32
Gain (dBi)	-2.38	-2.25	-1.21	0.12	1.28	4.02	3.59	3.88
Efficiency (dB)	-5.79	-6.08	-4.52	-4.14	-2.23	-1.33	-0.47	-0.44
Efficiency (%)	26.38	24.64	35.33	38.59	59.89	73.56	89.74	90.3

Frequency (MHz)	1750	1800	1850	1900	1950	2000	2150	2200
Directivity (dBi)	4.37	4.66	4.32	4.5	4.14	4.3	4.54	4.57
Gain (dBi)	4.46	4.61	4.55	4.98	4.37	3.35	4.32	3.22
Efficiency (dB)	0.09	-0.05	0.23	0.48	0.23	-0.95	-0.22	-1.35
Efficiency (%)	102.19	98.87	105.42	111.64	105.49	80.35	95.09	73.23

Frequency (MHz)	825	925	2300
Directivity (dBi)	3.06	3.61	4.38
Gain (dBi)	-2.38	-0.99	3.1
Efficiency (dB)	-5.44	-4.6	-1.28
Efficiency (%)	28.6	34.66	74.51

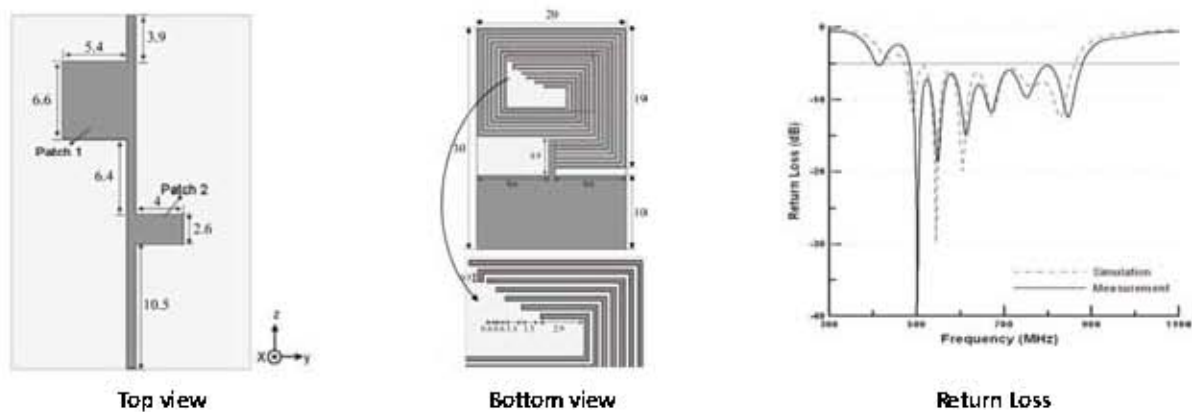
Measured gain data.

## ■ Spiral and Multimode Antenna Miniaturization for DTV Signal Receptions

D.-B. Lin, P.-C. Tsai, I.-T. Tang, and P.-S. Chen

*IEEE Antennas Wireless Propag. Lett.*, vol. 9, pp. 902 – 905, 2010.

A miniaturized spiral multimode antenna for encompassing the entire DTV signal reception bandwidth has been proposed. This antenna is composed of a microstrip, seven spiral lines, and a tuning pad. The volume of the antenna is only  $240 \text{ mm}^3$  ( $30 \times 20 \times 0.4 \text{ mm}^3$ ). The antenna is especially suited for application in small-sized DTV signal receptions and handheld mobile devices. The proposed antenna is easy to be integrated with radio-frequency/microwave circuitry for low manufacturing cost. The antenna also shows good radiation characteristics over the operating band. Furthermore, omnidirectional or near-omnidirectional radiation in the  $xy$ ,  $xz$ , and  $yz$  planes was also obtained. These are attractive features for practical applications over the entire DTV signal reception bandwidth.



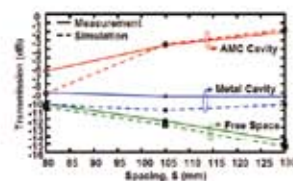
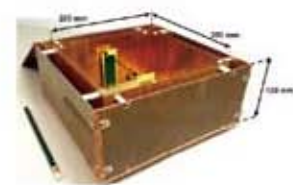
## Microwave/Millimeter Wave Systems

### ■ Coupling Enhancement Between Monopole-Type Resonators Using Metamaterial Cavity

C.-Y. Liou, C.-J. Kuo, M.-L. Lee and S.-G. Mao

*Appl. Physics Lett.*

This work presents the strong coupling of monopole-type resonators using a metamaterial cavity with artificial magnetic conductor (AMC) surfaces and metal planes. The AMC surface is constructed by an array of metal patches on a double-layered dielectric substrate backed by a metallic plane, and its reflection phase with respect to the angle and the polarization of obliquely incident plane waves are characterized by the transmission-line model. The measured transmission power is  $-2\text{dB}$  when the resonator spacing is  $0.4\lambda$ . This demonstrates that the power transfer is enhanced significantly by metamaterial cavity compared to the metal cavity and free space,  $\lambda$ .

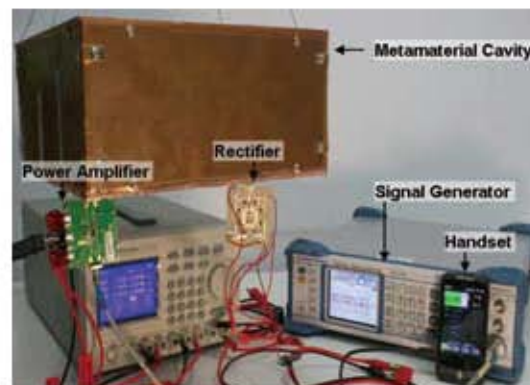


### ■ Wireless Charging System of Mobile Handset Using Metamaterial-Based Cavity Resonator

C.-Y. Liou, C.-J. Kuo, M.-L. Lee and S.-G. Mao

*IEEE MTT-S Int. Microw. Symp.*, June 2012.

A metamaterial-based cavity resonator using artificial magnetic conductor surfaces is presented and applied to realize a wireless charging system of mobile handset. This wireless charging system demonstrates the advantages of broad bandwidth, small size, long transmitting range, high transferring efficiency and EMI-free feature. The holistic architecture of wireless charging system for a smartphone is established to experimentally validate the usefulness of the metamaterial cavity resonator.

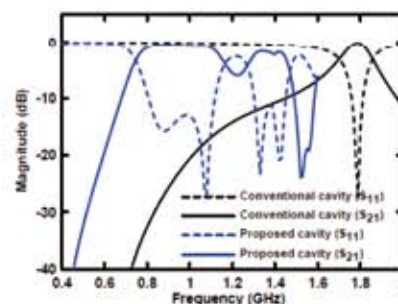
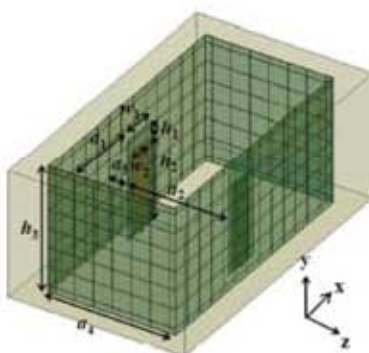


### ■ Novel Compact Metamaterial-Based Cavity Resonator with Broad Bandwidth

J.-C. Yeh, C.-Y. Liou, Y.-Z. Chueh, M.-S. Wu and S.-G. Mao

*IEEE AP-S. Int. Symp.*, Jul. 2010 [CD ROM]

This work describes a novel metamaterial-based cavity with a compact size. In contrast with the conventional cavity composed of six closed metal plates, the proposed metamaterial-based cavity is realized by integrating four AMC surfaces at the four sidewalls and two metal plates at the top and bottom walls. The AMC consists of a periodic array of square patches printed on the metal-backed double layer dielectric substrate to enhance its operating bandwidth. Two monopole-type antennas are used as the transmitting and receiving terminals in the proposed cavity. Owing to the reflected phase characteristics of the AMC surface, the cavity resulting in a more compact size and broader bandwidth than those of the conventional cavity.

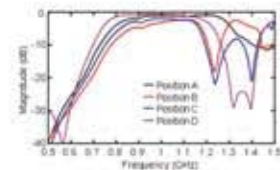
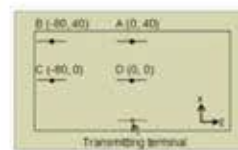
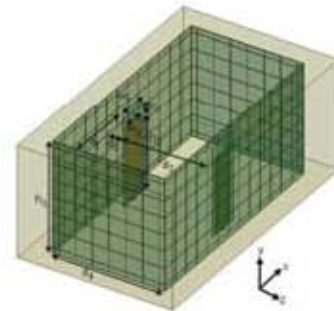


■ Broadband and Strong Coupling Metamaterial-Based Cavity Resonator Using Artificial Magnetic Surfaces

C.-Y. Liou, C.-J. Kuo, J.-C. Yeh, Y.-Z. Chueh, and S.-G. Mao

2011 IEEE MTT-S Int. Microw. Workshop Series on Innovative Wireless Power Transmission: Technol., Syst., Appl. (IMWS), pp.119-121, May 2011.

This study proposes a novel metamaterial-based cavity with a strong coupling effect between the transmitting and receiving devices. It is compact in size and the field distribution is uniform inside the cavity, which is realized by combining four artificial magnetic conductor surfaces at the four sidewalls and two metal plates at the top and bottom walls. The AMC consisting of a periodic array of square patches printed on the metal-backed double-layer dielectric substrate without connecting vias to enhance its operating bandwidth. Two monopole-type antennas are used as the transmitting and receiving terminals to examine the transmission property. The measured insertion loss of the metamaterial-based with different receiving positions are 1.06 dB, 2.26 dB, 2.02 dB, and 0.6 dB for position A, B, C, and D, respectively. The fabrication and measurement of the metamaterial-based cavity are demonstrated to validate its broad bandwidth and compact size.



- A novel RF sensing circuit using injection locking and frequency demodulation for cognitive radio applications

C.-J. Li, F.-K. Wang, T.-S. Horng, and K.-C. Peng

*IEEE Trans. Microw. Theory Tech.*, vol. 57, no. 12, pp. 3143–3152, Dec. 2009.

A novel RF sensing circuit for a cognitive radio to sense spectral environment is proposed based on injection locking and frequency demodulation techniques. In the experiments, a prototype circuit is designed in the 2.4 GHz ISM band to cover a sensing frequency range from 2.4 to 2.499 GHz. The spectrum scanning over the 99-MHz bandwidth is accomplished in 1 ms. The experimental results show that the RF sensing circuit can sense the frequency and the power of frequency-modulated signals as well as digitally modulated signals.

The presented RF sensing circuit is capable of sensing sinusoidal signals and modulation signals for cognitive radio applications with the sensitivity of 80 dBm and the frequency scanning speed of 100 MHz/ms, showing a more attractive performance versus complexity benefit than the usual approaches using a frequency synthesizer. In addition, the same circuit can also serve as a cognitive radio receiver supporting variable data rate under received-power constraints.

